Supporting Information

Highly efficient •OH generation in Fenton-like reactions over bioinspired manganese single-atom site

Man Yang*[,a] and Yujing Ren[b,c]

[a.] School of Materials Science and Engineering, Xi'an University of Technology, Xi'an 710048, China.

[b.] School of Life Sciences, Northwestern Polytechnical University, Xi'an, 710072, Shaanxi, China.

[c.] Chongqing Innovation Center, Northwestern Polytechnical University, Chongqing, 401135, China.

[*] To whom correspondence should be addressed. myang@xaut.edu.cn (M. Yang)

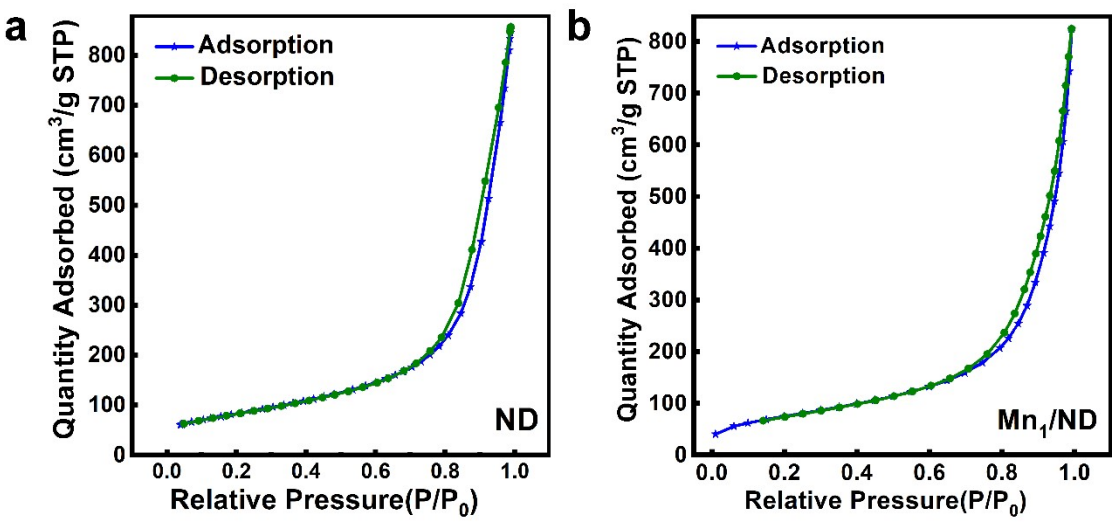

Figure S1. Nitrogen adsorption-desorption isotherm of (a) ND and (b) Mn_1/ND samples.

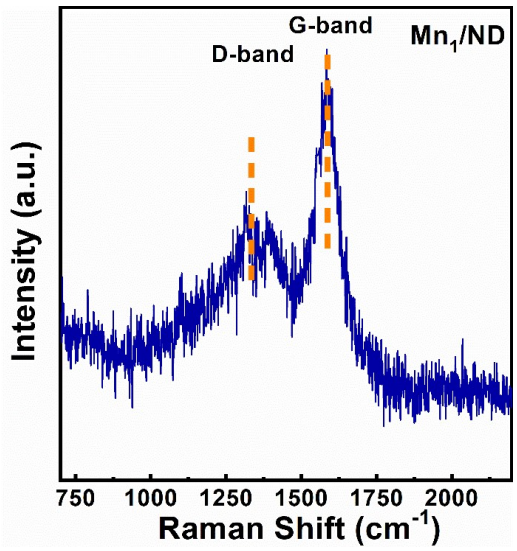

Figure S2. Raman result of and Mn_1/ND catalyst.

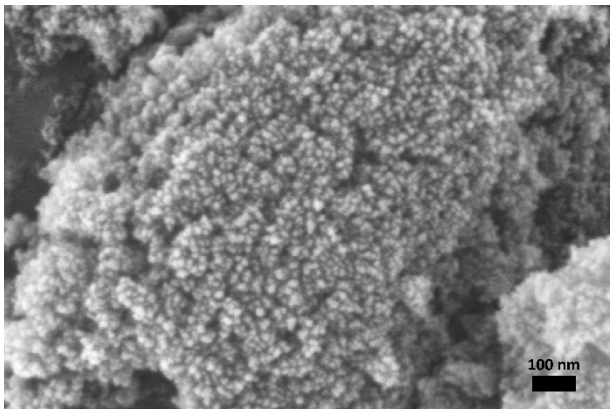

Figure S3. FESEM images of Mn_1/ND catalyst.

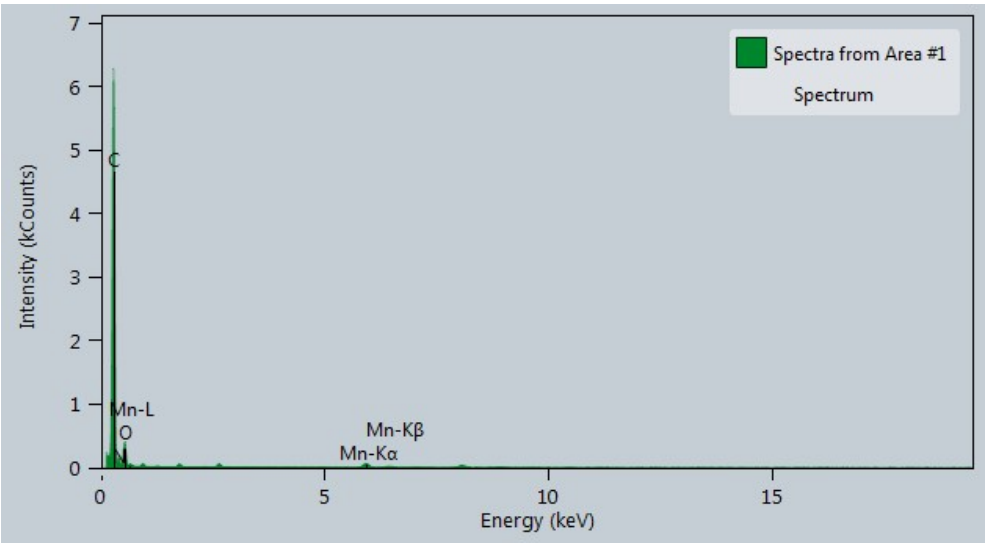

Figure S4. EDS spectra of Mn_1/ND sample.

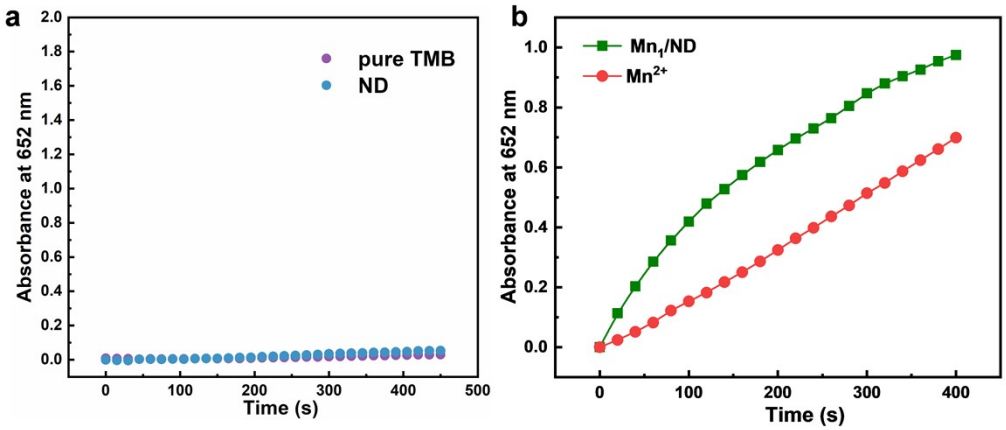

Figure S5. Peroxidase-like activity of TMB oxidation in different catalytic system.

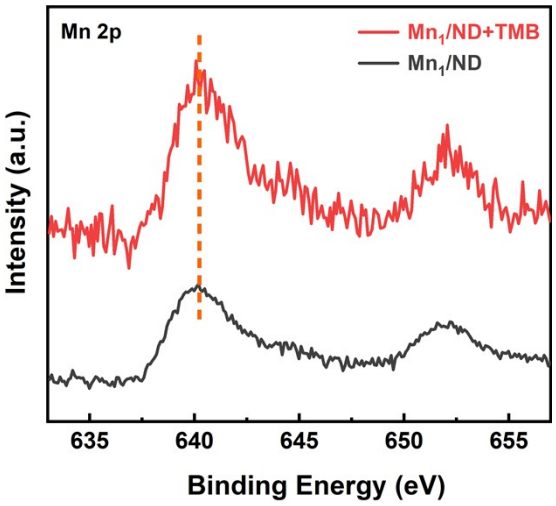

Figure S6. The XPS specrta of Mn 2p in Mn_1/ND+TMB sample.

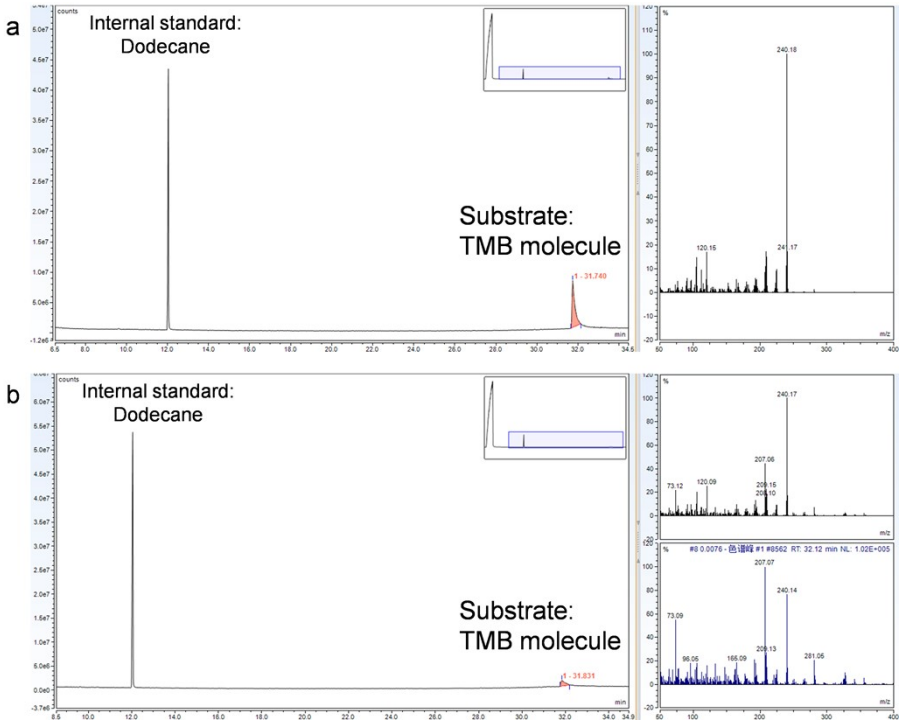

Figure S7. The GC-MS results of (a) blank experiment and (b) TMB adsorption on Mn_1-ND catalyst. After the normalization of internal standard intensity, it is obviously showed that the intensity of TMB molecule in Fig. S7b is much lower than that in Fig. S7a, which indicates that the TMB is adsorbed on the Mn_1-ND catalyst.

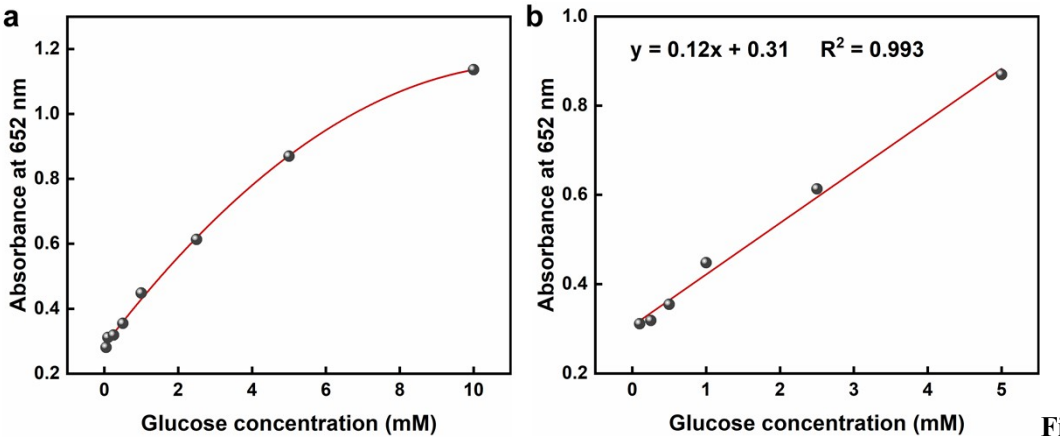

Figure S8. (a) Plots of peak absorbance values versus glucose concentration; (b) Linear calibration plot for glucose.

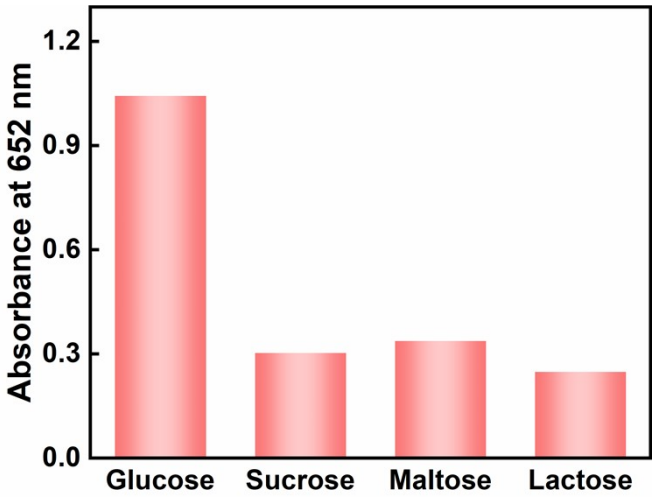

Figure S9. Specificity of the method. The glucose concentration was 1 mM. The concentrations of sucrose, maltose and lactose were 10 mM, respectively.

Table S1. ICP-OES results of Mn_1/ND catalyst.

Sample	M loading (wt%)
Mn_1/ND	1.15

Table S2. BET surface area of ND and Mn_1/ND samples.

Sample	S_{BET} (m^2/g)
ND	297.2
Mn_1/ND	272.8

Table S3. The mass fraction of Mn species from EDS spectra analysis.

Sample	Element	Family	Mass fraction (%)	Mass error (%)	Ratio of mass fraction to mass error
Mn_1/ND	Mn	K	1.77	0.24	7.3
	C+N+O	K	98.23	-	-

Table S4. N 1s XPS analysis results of ND and Mn_1/ND samples.

Sample	N species	Binding energy (eV)	Proportion (%) [a]	Surface $N_{(M-N)}$/Mn atomic ratio [b]
ND	Pyridinic N	398.4	81.3	-
	Graphitic N	401.9	18.7	-
Mn_1/ND	Pyridinic N	398.3	59.8	-
	M-N	399.8	20.9	4.3
	Graphitic N	402.4	19.3	-

[a] Proportion of the nitrogen species in all nitrogen.

[b] The surface N/Mn atomic ratio was calculated according to supplementary equation:

$$n_i/n_j = I_i/I_j \times \sigma_j/\sigma_i \times E_{kj}^{0.5}/E_{ki}^{0.5}$$

i: N species; j: Mn species; n: the numbers of surface atom; I: the intensity of XPS peak area;

σ: photoionization cross section;

$Al_{K\alpha}$: N 1s = 1.8, Mn $2p_{3/2}$ = 9.2;

E_k: photoelectron kinetic energy, $E_k = h\nu$ ($Al_{K\alpha}$, $h\nu$ = 1486.6 eV) – BE (Binding Energy);

Table S5. The best-fitted EXAFS results of Mn_1/ND catalyst.[a]

Sample	Shell	CN	R (Å)	σ^2 (10^{-2} Å^2)	ΔE_0 (eV)	r-factor (%)
Mn_1/ND	Mn-N	3.7	1.95	1.2	-10.0	0.6

[a] CN is the coordination number for the absorber-backscatterer pair, R is the average absorber-backscatterer distance, σ^2 is the Debye-Waller factor, and ΔE_0 the inner potential correction. For Mn K-edge EXAFS spectra fitting, the S_0^2 value is 0.95. The accuracies of the above parameters are estimated as CN, ±20%; R, ±1%; σ^2, ±20%; ΔE_0, ±20%. The data range used for data fitting in k-space (Δk) and R-space (ΔR) are 3.0-9.0 Å^{-1} and 1.0-2.0 Å, respectively.

Table S6. TOF of TMB oxidation over Mn_1/ND and reported catalysts.

Catalyst	TOF (min^{-1})	Ref
Mn_1/ND	9.6	This work
FeBNC	5.9	1
Fe-N-C SA	3.2	2
Fe SAEs	6.7	3
Co/A-TiO_2	1.1	4
Ni/MOF	0.003	5
aNiPc	0.014	6
Cu-HCSs	0.022	7

Table S7. DFT calculation results of the H_2O_2 adsorbed on Mn_1-N_4 site.

System	E_{ads} (eV)
Mn_1-N_4	-2.8 eV

Table S8. N 1s XPS analysis results of Mn_1/ND+TMB samples.

Sample	N species	Binding energy (eV)	Proportion (%) [a]
Mn_1/ND+TMB	Pyridinic N	398.3	43.5
	Adsorbed N	399.3	30.6
	M-N	399.9	15.3
	Graphitic N	403.0	10.6

[a] Proportion of the nitrogen species in all nitrogen.

Table S9. ICP-OES result of Mn_1/ND-spent catalyst.

Sample	M loading (wt%)
Mn_1/ND-spent	1.06

Reference

(1) Jiao, L.; Xu, W. Q.; Zhang, Y.; Wu, Y.; Gu, W. L.; Ge, X. X.; Chen, B. B.; Zhu, C. Z.; Guo, S. J. Boron-doped Fe-N-C single-atom nanozymes specifically boost peroxidase-like activity. *Nano Today* **2020**, *35*, 10.

(2) Jiao, L.; Xu, W.; Yan, H.; Wu, Y.; Zhu, C. Fe-N-C single-atom nanozyme for the intracellular hydrogen peroxide detection. *Anal. Chem.* **2019**, *91,*11994-11999.

(3) Zhao, C.; Xiong, C.; Liu, X.; Qiao, M.; Li, Y. Unraveling the single atomic active site under realistic simulated natural heme-containing enzymes. *Chem. Comm.* **2019**, *55*, 16.

(4) Wang, H.; Wang, Y.; Lu, L. L.; Ma, Q.; Feng, R. X.; Xu, S. Y.; James, T. D.; Wang, L. Y. Reducing valence states of Co active sites in a single-atom nanozyme for boosted tumor therapy. *Adv. Funct. Mater.* **2022**, *9,* 202200331.

(5) Chen, J. Y.; Shu, Y.; Li, H. L.; Xu, Q.; Hu, X. Y. Nickel metal-organic framework 2D nanosheets with enhanced peroxidase nanozyme activity for colorimetric detection of H_2O_2. *Talanta* **2018**, *189*, 254-261.

(6) Zhao, Y.; An, F. H.; Meng, J.; Zhu, Y. X.; Sun, X.; Zhang, X. M.; Sun, X. Nickel phthalocyanines as potential aggregation-induced antibacterial agents: Fenton-like pathways driven by near-infrared light. *ChemPhotoChem* **2022**, *6*, e202100233.

(7) Xi, J. Q.; Wei, G.; An, L. F.; Xu, Z. B.; Xu, Z. L.; Fan, L.; Gao, L. Z. Copper/carbon hybrid nanozyme: Tuning catalytic activity by the copper state for antibacterial therapy. *Nano Lett.* **2019**, *19*, 7645-7654.